Femtosecond solitons in nonlinear optical fibers: Classical and quantum effects

F. Singer, M. J. Potasek, J. M. Fang, and M. C. Teich
Departments of Physics, Applied Physics, and Electrical Engineering, Columbia University, New York, New York 10027
(Received 2 March 1992)

We use the time-dependent Hartree approximation to obtain solutions to a quantized higher-order nonlinear Schrödinger equation. This equation describes pulses propagating in nonlinear-optical fibers and, under certain conditions, has femtosecond soliton solutions. These solitons travel at velocities that differ from those of the picosecond solitons obtained from the standard quantized nonlinear Schrödinger equation. Furthermore, we find that quadruple-clad fibers are required for the propagation of these solitons, unlike the solitons of the standard nonlinear Schrödinger equation, which can propagate in graded-index optical fibers. From the quantum solution, we find that the soliton experiences phase spreading and self-squeezing as it propagates.

PACS number(s): 42.50.Dv, 42.50.Rh, 42.81.Dp, 42.65.Re

I. INTRODUCTION

There is considerable interest in nonlinear-dynamical processes in terms of both classical and quantum phenomena [1–11]. Early theoretical work investigated quadrature squeezing for the nonlinear Schrödinger equation (NLS) assuming a continuous-wave input; it was observed that the squeezing was enhanced in the anomalous dispersion region [3]. Drummond and Carter used a numerical technique to investigate quadrature squeezing for solitons in optical fibers [4]. Rosenbluh and Shelby have experimentally demonstrated this squeezing [5]. Kitagawa and Yamamoto [6], and also Tanas and Kielich [7], investigated number-phase minimum-uncertainty states for self-phase modulation (SPM) in a Kerr medium. Kennedy and Drummond have developed exact theories describing the quantum-statistical properties of a continuous wave including SPM [8]. Further analytical results were obtained by Yurke and Potasek for the initial value problem for the quantum NLS using the Gutkin formalism [9]. However, this applied to pulses in the normal dispersion region where bright solitons cannot form. Lai and Haus developed a quantum theory of solitons in optical fibers using the time-dependent Hartree approximation and also using Bethe's ansatz [10]. Wright further investigated the theory using the time-dependent Hartree approximation by considering the case of a pulse whose initial profile is the classical solution [11].

However, the NLS is generally not valid for pulses with durations shorter than the picosecond time scale. Yet the recent development of optical sources that generate pulses in the femtosecond domain makes possible the exploration of many phenomena [12]. Therefore the investigation of solitons arising from the higher-order NLS (HNLS), which can be used in the femtosecond time domain, are of interest. We use the time-dependent Hartree approximation to develop a quantum theory of femtosecond solitons. We compare this to the NLS theory and discuss the applicability of this solution to optical fibers. We find that the graded-index fibers used by Rosenbluh and Shelby for their initial experiment cannot be used for our case of femtosecond solitons. Rather, the higher-order dispersion term must be negative, requiring a quadruple-clad fiber [13]. Using the numerical beam propagation method (NBP), we examine the propagation of classical solitons for various parameters and observe that the higher-order terms affect the velocity of the soliton relative to the group velocity obtained from the NLS. Furthermore, we use the NBP to show that on the scale at which the quantum behavior is of interest, the effects of the soliton self-frequency shift can be neglected.

Assuming an initial coherent state, we calculate the quasiprobability density and plot its behavior as a function of distance along the fiber. As with the NLS, self-squeezing occurs as the soliton propagates. However, in our case the distance at which self-squeezing occurs is shorter than that for the NLS, partly because of the shorter pulses required.

II. CLASSICAL ANALYSIS

The general equation describing the propagation of femtosecond pulses in nonlinear optical fibers is given by [14,15]

$$i\frac{\partial\phi}{\partial t}+\frac{\partial^2\phi}{\partial x^2}+2C|\phi|^2\phi+id\frac{\partial^3\phi}{\partial x^3}+i\epsilon_1 C|\phi|^2\frac{\partial\phi}{\partial x}+i\epsilon_2 C|\phi|^2\frac{\partial\phi^*}{\partial x}-\epsilon_3 C\phi\frac{\partial|\phi|^2}{\partial x}=0\ , \quad (1)$$

where C, d, ϵ_1, ϵ_2, and ϵ_3 are constants and ϕ represents the normalized envelope of the electromagnetic field. We follow the conventional notation in the mathematical literature, which uses t and x to represent normalized space and time, respectively. The time variable x is normalized by the group velocity defined by $(v_g)^{-1}=\partial\beta/\partial\omega|_{\omega_0}$. The quantities C, d, ϵ_1, ϵ_2, and ϵ_3 are given by

$$C \equiv \frac{n_2 \omega_0 \sigma^2 I^2}{c|\beta_2|} ,$$
$$d \equiv \frac{|\beta_3|}{3\sigma|\beta_2|} ,$$
$$\epsilon_1 \equiv \frac{4}{\sigma}\left[\frac{2}{\omega_0}+\frac{n'}{n}+\frac{3h'}{h}\right] , \quad (2)$$
$$\epsilon_2 \equiv \frac{2}{\sigma}\left[\frac{2}{\omega_0}+\frac{n'}{n}+\frac{4h'}{h}\right] ,$$
$$\epsilon_3 \equiv 2\frac{T_R}{\sigma} .$$

β_2 and β_3 are dispersion parameters given by the second and third derivatives of the propagation constant with respect to frequency, respectively, evaluated at the carrier frequency ω_0 and for bright solitons we have found that both must be negative. n is the linear index of refraction, n_2 is the nonlinear index of refraction, σ is the $1/e$ width of the pulse intensity, h is the frequency-dependent radius of the fiber mode, I is the peak amplitude of the pulse, and c is the speed of light. Primes denote the derivative with respect to frequency and all parameters are evaluated at ω_0. T_R is a parameter related to the slope of the Raman gain curve [16].

Equation (1) reduces to the NLS for $d=\epsilon_1=\epsilon_2=\epsilon_3=0$. When $\epsilon_2=\epsilon_3=0$ and $\epsilon_1=6d$ Eq. (1) gives rise to a HNLS of the form

$$i\frac{\partial\phi}{\partial t}+\frac{\partial^2\phi}{\partial x^2}+2C|\phi|^2\phi+id\left[\frac{\partial^3\phi}{\partial x^3}+6C|\phi|^2\frac{\partial\phi}{\partial x}\right]=0 . \quad (3)$$

This equation has soliton solutions [14]. The effects of the soliton self-frequency shift (SSFS) [16] (the ϵ_3 term), and the ϵ_2 term, on the solution of Eq. (3) will be discussed in Sec. IV using the NBP. The SSFS is a continuous downshift of the mean frequency of subpicosecond pulses. It has been explained in terms of the Raman effect through which the soliton can self-induce gain for the lower-frequency part of its spectrum at the expense of the higher-frequency part [16]. This effect has been observed experimentally [17]. We focus on Eq. (3) to examine the soliton properties.

The general solution of Eq. (3) has the form [14]

$$\phi=\phi_0 \mathrm{sech}[\epsilon(x-x_0)+\beta t]\exp\{i[\gamma(x-x_0)+\delta t]\} , \quad (4)$$

where ϵ, β, γ, and δ are constants and x_0 is the zero of time. Substituting this in Eq. (3) yields the following relations:

$$|\phi_0|^2=\frac{\epsilon^2}{C} ,$$
$$\delta=\epsilon^2-\gamma^2-3d\gamma\epsilon^2+d\gamma^3 , \quad (5)$$
$$\beta=\epsilon(2\gamma+d\epsilon^2-3d\gamma^2) .$$

These results will be used in later sections of the paper.

III. QUANTUM ANALYSIS

In this section we use the time-dependent Hartree approximation to obtain the quantized HNLS and compute the quasiprobability density function [18]. We proceed by considering the quantum version of Eq. (3) from a mathematical point of view. The initial portion of our analysis closely follows that of Lai and Haus [10] for the NLS. To obtain the quantum version of Eq. (3), the quantities $\phi(t,x)$ and $\phi^*(t,x)$ are replaced by the field operators $\hat{\phi}(t,x$ and $\hat{\phi}^\dagger(t,x)$, which satisfy the boson commutation relations

$$[\hat{\phi}(t,x'),\hat{\phi}^\dagger(t,x)]=\delta(x-x') ,$$
$$[\hat{\phi}(t,x'),\hat{\phi}(t,x)]=[\hat{\phi}^\dagger(t,x'),\hat{\phi}^\dagger(t,x)]=0 , \quad (6)$$

where $\hat{\phi}(t,x)$ and $\hat{\phi}^\dagger(t,x)$ are the photon annihilation and creation operators, respectively, at t and x.

The quantized equation can be written as

$$i\hbar\frac{\partial}{\partial t}\hat{\phi}(t,x)=[\hat{\phi}(t,x),\hat{H}] , \quad (7)$$

with

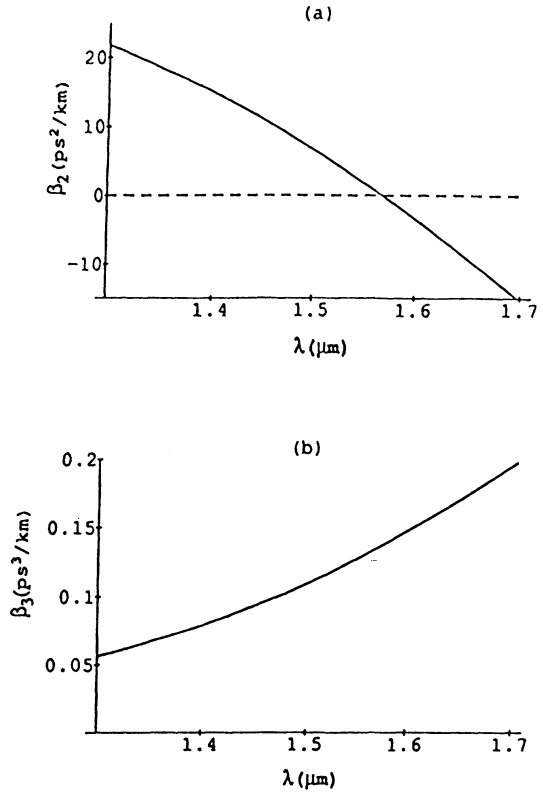

FIG. 1. Plots of β_2 and β_3 vs wavelength λ for a typical graded-index fiber.

$$\hat{H}=\hbar\left\{\int\hat{\phi}_x^\dagger(t,x)\hat{\phi}_x(t,x)dx-C\int\hat{\phi}^\dagger(t,x)\hat{\phi}^\dagger(t,x)\hat{\phi}(t,x)\hat{\phi}(t,x)dx\right.$$
$$\left.+id\left[\int\hat{\phi}_x(t,x)\hat{\phi}_{xx}(t,x)dx-3C\int\hat{\phi}^\dagger(t,x)\hat{\phi}^\dagger(t,x)\hat{\phi}(t,x)\hat{\phi}_x(t,x)dx\right]\right\}, \tag{8}$$

where the subscripts x and xx signify differentiation and double differentiation, respectively.

In the Schrödinger picture, the state of the system $|\Psi\rangle$ evolves according to

$$i\hbar\frac{\partial}{\partial t}|\Psi\rangle=\hat{H}_s|\Psi\rangle\ , \tag{9}$$

where

$$\hat{H}_s=\hbar\left\{\int\hat{\phi}_x^\dagger(x)\hat{\phi}_x(x)dx-C\int\hat{\phi}^\dagger(x)\hat{\phi}^\dagger(x)\hat{\phi}(x)\hat{\phi}(x)dx\right.$$
$$\left.+id\left[\int\hat{\phi}_x(x)\hat{\phi}_{xx}(x)dx-3C\int\hat{\phi}^\dagger(x)\hat{\phi}^\dagger(x)\hat{\phi}(x)\hat{\phi}_x(x)dx\right]\right\}. \tag{10}$$

In general, any state of this system can be expanded in Fock space as

$$|\Psi\rangle=\sum_n a_n\int\frac{1}{\sqrt{n!}}f_n(x_1,\ldots,x_n,t)\hat{\phi}^\dagger(x_1)\cdots\hat{\phi}^\dagger(x_n)dx_1\cdots dx_n|0\rangle\ . \tag{11}$$

The quantity $|a_n|^2$ is the probability of finding n photons in the field and we require

$$\sum_n|a_n|^2=1\ . \tag{12}$$

f_n obeys the normalization condition

$$\int|f_n(x_1,\ldots,x_n,t)|^2dx_1\cdots dx_n=1\ . \tag{13}$$

Substituting Eqs. (10) and (11) into (9) we obtain

$$i\frac{\partial}{\partial t}f_n(x_1,\ldots,x_n,t)=\left[-\sum_{j=1}^n\frac{\partial^2}{\partial x_j^2}-2C\sum_{1\le i<j\le n}\delta(x_j-x_i)\right.$$
$$\left.-id\sum_{j=1}^n\frac{\partial^3}{\partial x_j^3}-6iCd\sum_{1\le i<j\le n}\delta(x_j-x_i)\frac{\partial}{\partial x_j}\right]f_n(x_1,\ldots,x_n,t)\ . \tag{14}$$

We solve Eq. (14) using the time-dependent Hartree approximation [19]. We define a Hartree wave function

$$f_n^{(H)}(x_1,\ldots,x_n,t)=\prod_{j=1}^n\Phi_n(x_j,t)\ , \tag{15}$$

where Φ_n has the normalization

$$\int|\Phi_n(x,t)|^2dx=1\ . \tag{16}$$

The functions Φ_n are determined by minimizing the functional

$$I=\int f_n^{*(H)}(x_1,\ldots,x_n,t)\left\{i\frac{\partial}{\partial t}+\sum_{j=1}^n\left[\frac{\partial^2}{\partial x_j^2}+id\frac{\partial^3}{\partial x_j^3}\right]+\sum_{1\le i<j\le n}\delta(x_j-x_i)\left[2C+6iCd\frac{\partial}{\partial x_j}\right]\right\}$$
$$\times f_n^{(H)}(x_1,\ldots,x_n,t)dx_1\cdots dx_n\ , \tag{17}$$

which provides

$$i\frac{\partial\Phi_n}{\partial t}+\frac{\partial^2\Phi_n}{\partial x^2}+2C(n-1)|\Phi_n|^2\Phi_n+id\frac{\partial^3\Phi_n}{\partial x^3}+6iCd(n-1)|\Phi_n|^2\frac{\partial\Phi_n}{\partial x}=0\ . \tag{18}$$

This is identical to the classical HNLS given in Eq. (3), with C replaced by $C(n-1)$. Thus the solution to the quantized femtosecond soliton equation is obtained directly from Eqs. (4) and (5),

$$\Phi_n(x,t)=[C(n-1)]^{-1/2}\epsilon\,\mathrm{sech}\{\epsilon[(x-x_0)+(-3d\gamma^2+d\epsilon^2+2\gamma)t]\}$$
$$\times\exp[-i(-d\gamma^3+3d\gamma\epsilon^2+\gamma^2-\epsilon^2)t+i\gamma(x-x_0)]\ . \tag{19}$$

The normalization condition, Eq. (12), gives

$$\epsilon=\frac{n-1}{2}C\ . \tag{20}$$

Substituting Eq. (20) into Eq. (19) leads to

$$\Phi_{n\gamma}(x,t)=\frac{(n-1)^{1/2}}{2}C^{1/2}\mathrm{sech}\left\{\frac{(n-1)}{2}C\left[(x-x_0)+\left[-3d\gamma^2+d\frac{(n-1)^2}{4}C^2+2\gamma\right]t\right]\right\}$$
$$\times\exp\left\{\left[id\gamma^3-i\tfrac{3}{4}d\gamma(n-1)^2C^2-i\gamma^2+i\frac{(n-1)^2}{4}C^2\right]t+i\gamma(x-x_0)\right\}\ . \tag{21}$$

The Hartree product eigenstates are, using Eqs. (11) and (15),

$$|n,\gamma,t\rangle_H=\frac{1}{\sqrt{n!}}\left[\int\Phi_{n\gamma}(x,t)\hat{\phi}^\dagger(x)dx\right]^n|0\rangle\ . \tag{22}$$

A superposition of these states, using a Poissonian distribution of n for a coherent-state pulse, gives

$$|\Psi_s\rangle_H=\sum_n\frac{\alpha_0^n}{n!}e^{-|\alpha_0|^2/2}\left[\int\Phi_{n\gamma}(x,t)\hat{\phi}^\dagger(x)dx\right]^n|0\rangle\ , \tag{23}$$

where $|\alpha_0|^2=n_0$ is the mean photon number.

The quasiprobability density (QPD) for the amplitude of the envelope of the field is defined as

$$Q(\alpha,x,t)\equiv|\langle\alpha,x|\Psi_s\rangle|^2\ , \tag{24}$$

where

$$|\alpha,x\rangle\equiv e^{-|\alpha|^2/2}\sum_{n=0}^{\infty}\frac{\alpha^n}{n!}[\hat{\phi}^\dagger(x)]^n|0\rangle \tag{25}$$

is the local coherent state at the time x. Substituting Eq. (23), with Eqs. (21) and (25), into Eq. (24) gives

$$Q(\alpha,x,t)=e^{-|\alpha|^2-|\alpha_0|^2}\left|\sum_{n=0}^{\infty}\frac{(\alpha^*\alpha_0)^n}{n!}\left\{\frac{(n-1)^{1/2}}{2}C^{1/2}\mathrm{sech}\left\{\frac{n-1}{2}C\left[(x-x_0)+\left[-3d\gamma^2+d\frac{(n-1)^2}{4}C^2+2\gamma\right]t\right]\right\}\right\}^n\right.$$
$$\left.\times\exp\left[\left[ind\gamma^3-in(n-1)^2\tfrac{3}{4}d\gamma C^2-in\gamma^2+in\frac{(n-1)^2}{4}C^2\right]t+i\gamma n(x-x_0)\right]\right|^2\ . \tag{26}$$

IV. DISCUSSION

In this section we discuss the physical parameters for these solitons and, using the numerical beam propagation method to solve Eq. (1), we show directly the propagation of these solitons for various experimental parameters. For the quantum effects, we plot the QPD as a function of distance and demonstrate self-squeezing; we also discuss the relationship of our solution to that of the NLS.

A. Classical effects

We first discuss the applicability of the classical solution to optical fibers. To evaluate the parameter d we

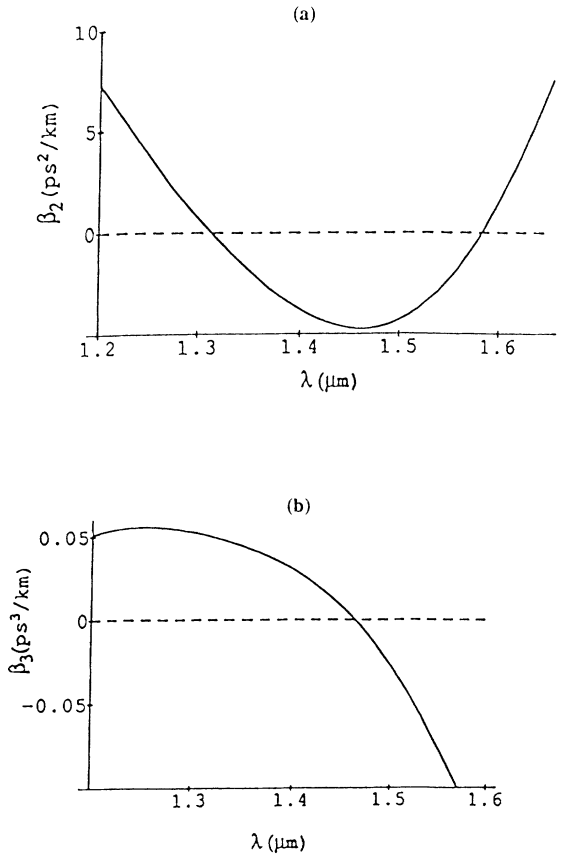

FIG. 2. Plots of β_2 and β_3 vs wavelength λ for a quadruple-clad fiber.

need values for β_2 and β_3. Figure 1 shows plots of β_2 and β_3 as a function of wavelength for a graded-index fiber when the transverse field is modeled by a Gaussian function [20]. β_3 is evaluated by taking the derivative with respect to frequency of the β_2 curve. Since β_3 is always positive this type of fiber is not suitable for supporting these bright solitons (β_2 and β_3 must both be negative to support bright solitons). This is significant inasmuch as graded-index fibers are traditionally used in calculations and experiments.

We next consider the quadruple-clad fiber. These fibers were developed to have two zero-dispersion wavelengths in two regions with relatively low loss: at about 1.3 and about 1.55 μm. We use experimental results [13] for β_2 to evaluate β_3. Plots of β_2 and β_3 are shown in Fig. 2. In these fibers β_3 does become negative above a certain wavelength as required for our solution. In Fig. 3 we show plots of $d'=\beta_3/3\sigma|\beta_2|$ for various values of the pulse width. The parameter d in our equations is related to d' by $d=|d'|$ [see Eq. (2)]. The parameter ϵ_1 in Eq. (2) also varies with pulse width and becomes significant only in the femtosecond regime [15]. In Fig. 4 we show a plot of $\log\epsilon_1$ versus the universal frequency V where $V=(2\Delta)^{1/2}\omega_0 na/c$, with a the geometric core radius and Δ the normalized index of refraction difference between the core and the cladding. The V number is an often-used optical-fiber parameter [13]. We use the usual wavelength $\lambda=1.55$ μm, which corresponds to an angular frequency $\omega_0=1.2\times10^{15}$ rad/sec. Using experimental parameters and numerical analysis we have found that in the wavelength region of 1.5–1.55 μm, ϵ_1 is fairly constant [20]. The parameter d, on the other hand, varies

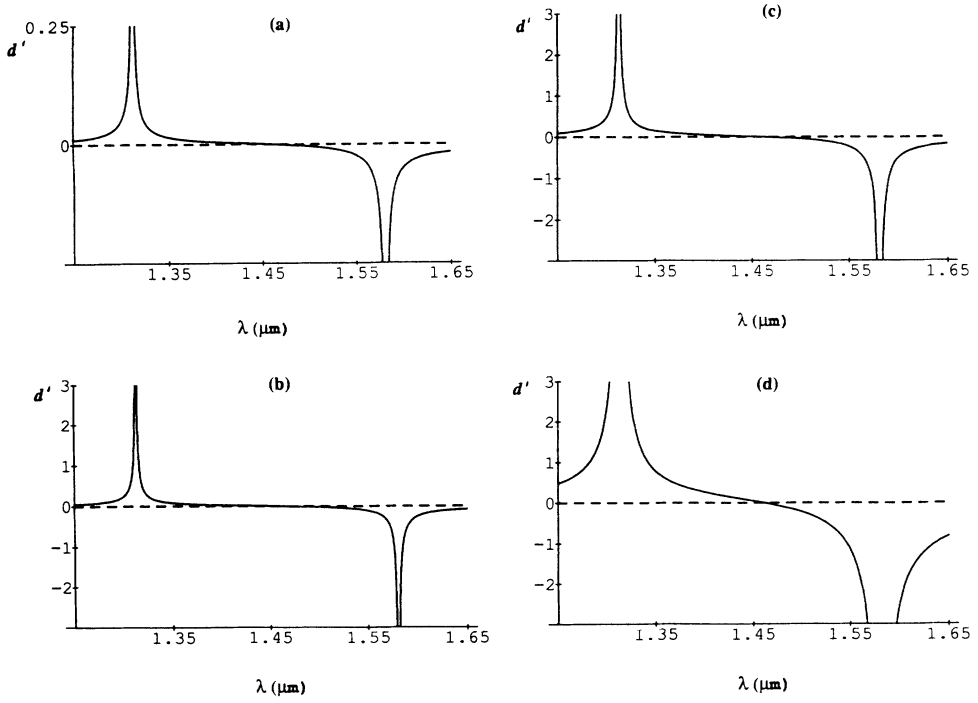

FIG. 3. Plots of d' vs wavelength λ for quadruple-clad fiber for σ values of (a) 500 fs, (b) 100 fs, (c) 50 fs, and (d) 10 fs.

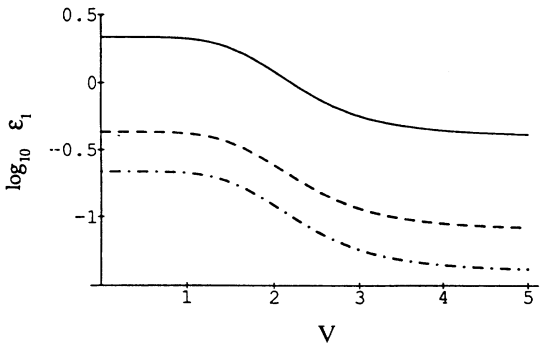

FIG. 4. Plot of $\log\epsilon_1$ as a function of the fiber V number assuming $\lambda=1.55$ μm. The solid curve corresponds to $\sigma=10$ fs, the dashed curve corresponds to $\sigma=50$ fs, and the dotted-dashed curve corresponds to $\sigma=100$ fs.

most significantly in this wavelength region, as can be seen in Fig. 3.

Next we use the NBP to investigate soliton propagation. We wish to verify our solution and to show that the other higher-order terms not included in Eq. (3), i.e., the ϵ_2 and ϵ_3 terms in Eq. (1), do not affect the soliton on the distance scale that quantum effects occur. The parameter d affects the velocity of the pulse. Numerical calculations of intensity as a function of time and distance t, and their corresponding contour plots for $d=0.25$ and for $d=0.5$, are shown in Fig. 5. As d increases the velocity decreases and shifts further from the group velocity as defined for the NLS. These calculations are in agreement with analytical results.

In addition, we use the NBP to investigate the other higher-order terms in Eq. (1). For these calculations we use the parameters $d=0.5$ and 0.25, and $\sigma\approx 50$ fs. We first look at the ϵ_2 term. Using the NBP we calculate both the time and frequency spectra of the soliton including this term with $\epsilon_2=0.5\epsilon_1$. For typical parameters this is a reasonable relationship [20]. These plots are shown in Fig. 6 for $d=0.25$ and in Fig. 7 for $d=0.5$. We find that this term does not substantially alter the soliton properties on the distance scale used for our QPD plots. For $\lambda=1.55$ μm, $\beta_2\approx -2.5$ ps^2/km, $\sigma=50$ fs, and $d=0.25$, $t=1$ corresponds to 2 m. This is in contrast with the NLS case with $\sigma=5$ ps for which $t=1$ corresponds to 20 m.

Similar calculations including the SSFS (ϵ_3 term) in place of the ϵ_2 term are shown in Fig. 8 for $d=0.25$ and in Fig. 9 for $d=0.5$. For optical fibers at $\lambda=1.55$ μm, $T_R\approx 6$ fs [16]. We find that this effect, too, does not substantially alter the soliton on the distance scale used for our plots. Alternatively, the SSFS may be compensated for by bandwidth-limited amplification as recent classical results have shown [21,22]. However, the amplification terms complicate the quantum calculations and are beyond the scope of our initial work. Recently, a quantum theory of propagation in fibers for a NLS modified to incorporate the Raman effect has been developed for picosecond pulses [23].

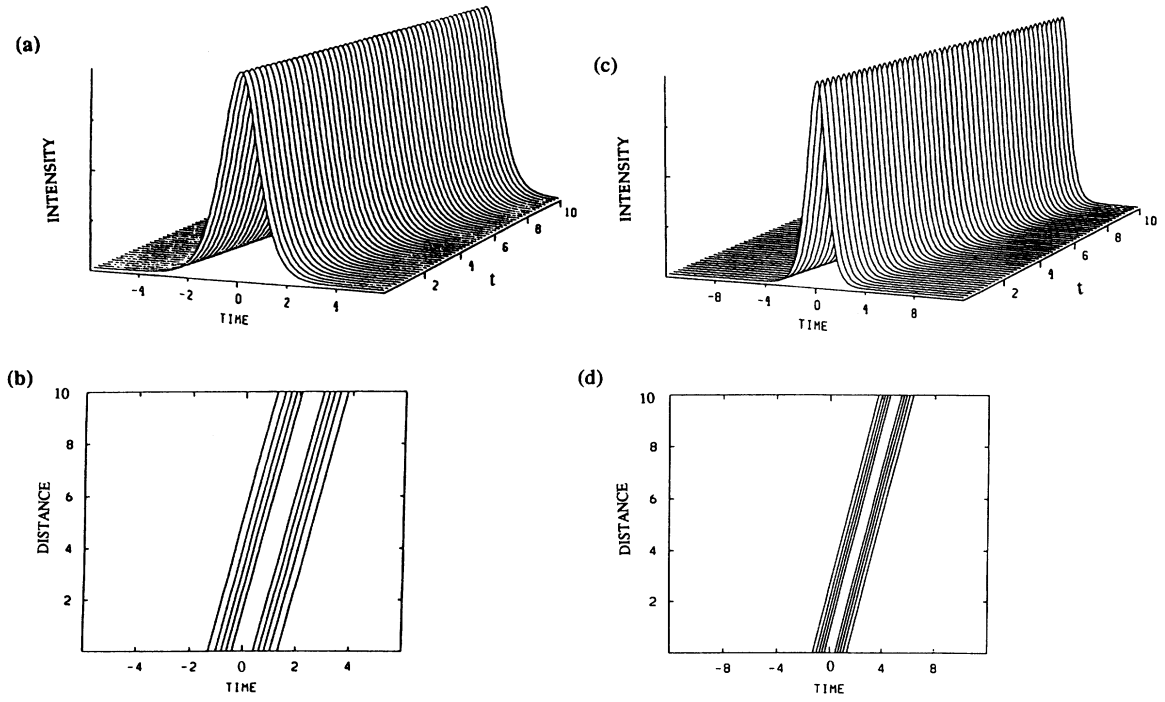

FIG. 5. (a) Numerical calculations of time and distance vs intensity and (b) the corresponding contour plot for $d=0.25$; (c) numerical calculations of time and distance vs intensity and (d) the corresponding contour plot for $d=0.5$.

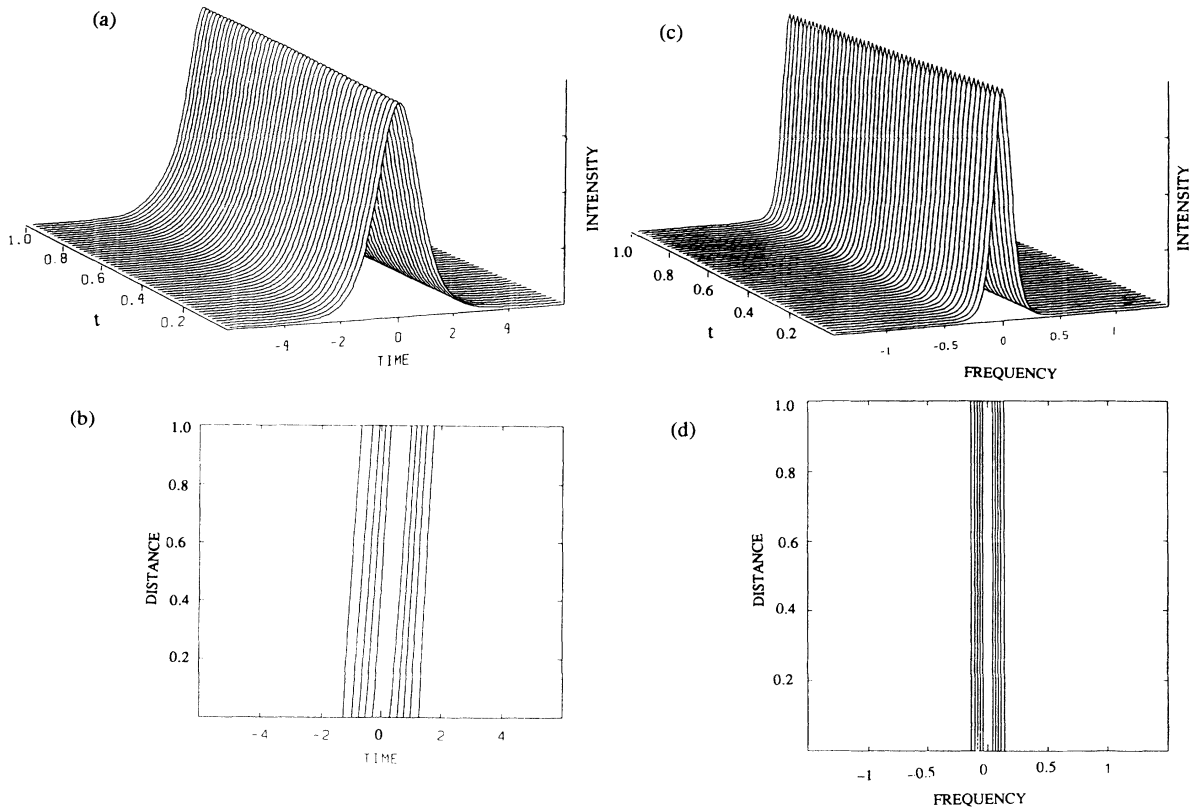

FIG. 6. Numerical calculations for the HNLS with $\epsilon_2=0.5\epsilon_1$ for $d=0.25$: (a) propagation as a function of distance and (b) the corresponding contour plot; (c) frequency spectrum as a function of distance and (d) the corresponding contour plot.

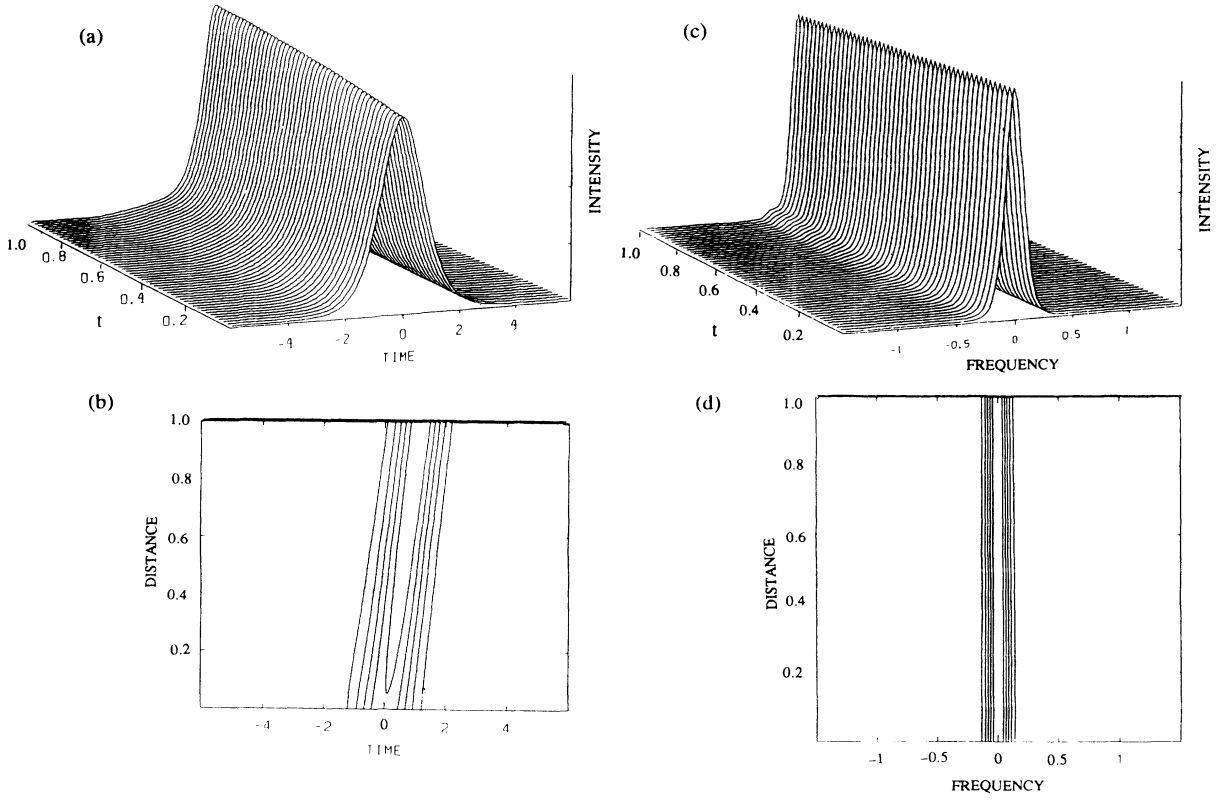

FIG. 7. Numerical calculations for the HNLS with $\epsilon_2=0.5\epsilon_1$ term for $d=0.5$: (a) propagation as a function of distance and (b) the corresponding contour plot; (c) frequency spectrum as a function of distance and (d) the corresponding contour plot.

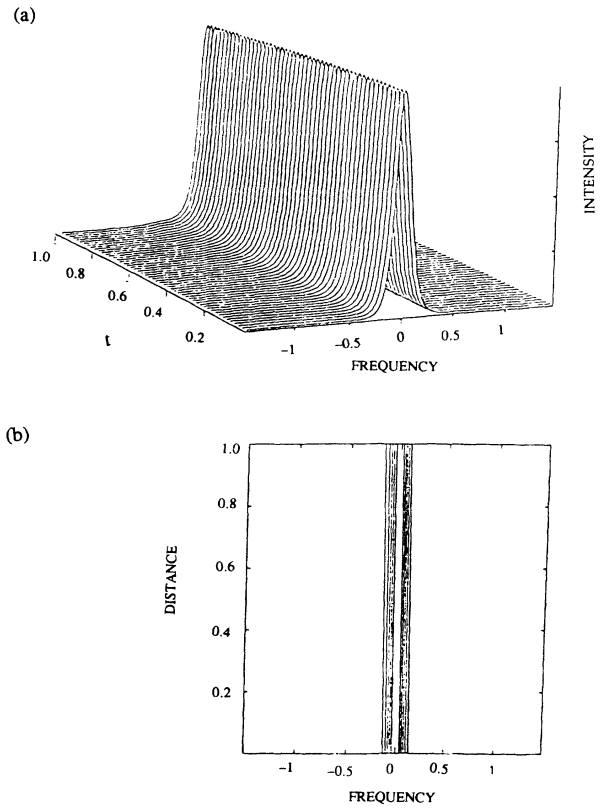

FIG. 8. Numerical calculations for the HNLS including the SSFS (ϵ_3 term) for $d=0.25$: (a) frequency spectrum as a function of distance and (b) the corresponding contour plot.

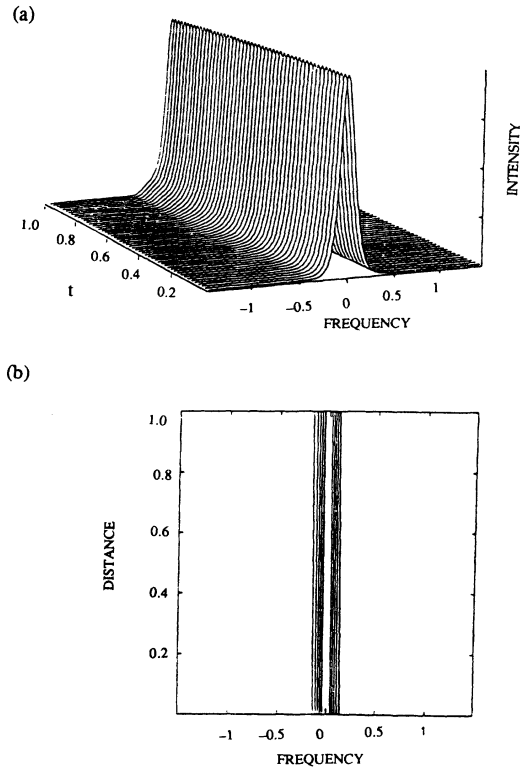

FIG. 9. Numerical calculations for the HNLS including the SSFS term for $d=0.5$: (a) frequency spectrum as a function of distance and (b) the corresponding contour plot.

B. Quantum effects

In this section we will use the results from Sec. III. For simplicity, we ignore the n dependence of the amplitude in Eq. (25) and replace n by n_0. In Figs. 10 and 11 we show plots of Q with $d=0.25$ for increasing distance t. Figure 10 shows the initial state at $t=0$, which is a coherent state. As can be seen in Figs. 11(a) and 11(b), as t increases the phase spreads and the soliton becomes self-squeezed. As we increase t further and the phase spreading increases, the distribution begins to overlap itself and gives the appearance of interference as shown in Figs. 10(c) and 10(d). To follows the center of the pulse as t increases we must change x accordingly to keep the argument of the sech term constant. The effects observed in the HNLS case are qualitatively the same as those in

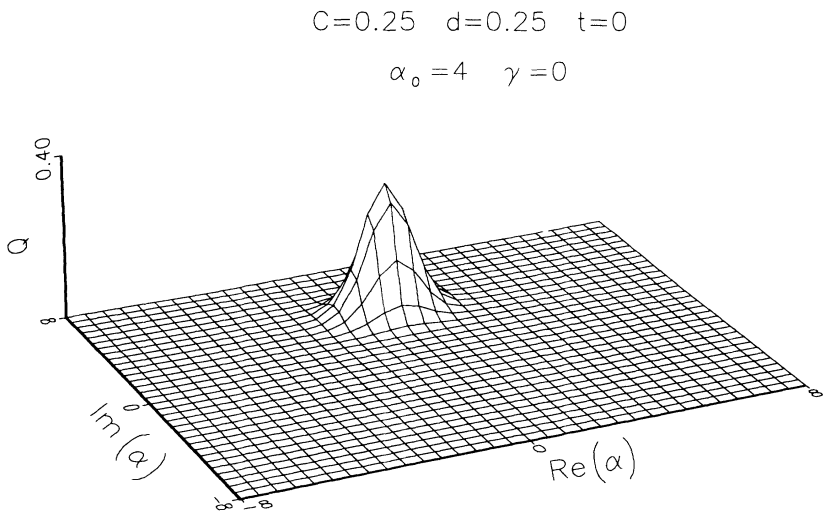

FIG. 10. Plot of the quasiprobability density $Q(\alpha,x,t)$ vs the real and imaginary parts of α for $\alpha_0=4$, $C=0.25$, $\gamma=0$, $(x-x_0)=0$, $d=0.25$, and $t=0$.

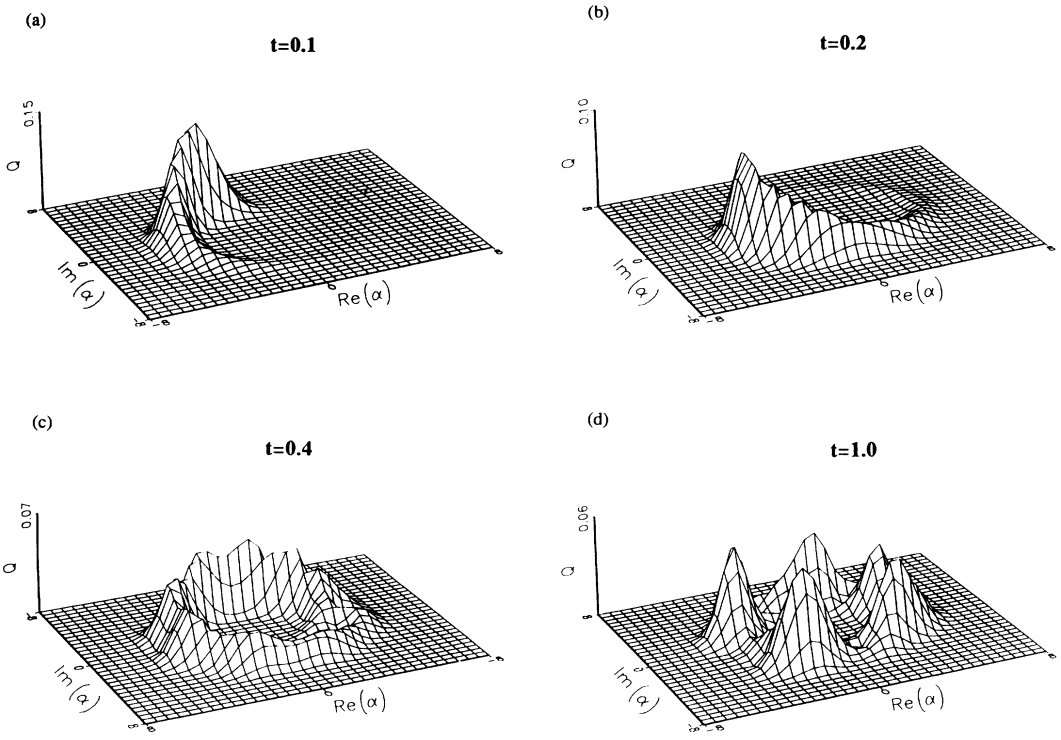

FIG. 11. Plots of the quasiprobability density $Q(\alpha,x,t)$ vs the real and imaginary parts of α for $\alpha_0=4$, $C=0.25$, $\gamma=0$, $(x-x_0)=0$, and $d=0.25$ with several values of t: (a) $t=0.1$, (b) $t=0.2$, (c) $t=0.4$, (d) $t=1$.

the NLS case [10,11]. However, as a result of the higher-order terms these effects occur at different distances along the fiber. Since d is a function of wavelength and varies significantly in the region around 1.55 μm, we can choose the operating wavelength that provides the effect we desire, i.e., more or less squeezing.

In addition, our solution in Eq. (4) allows for the possibility of an additional frequency shift to the soliton by having γ nonzero. This is equivalent to frequency-shifting the soliton before it enters the fiber and would have the effect of slowing down or speeding up the phase spreading depending on whether the frequency was shifted up or down. This may be accomplished experimentally by using an acoustic-optic modulator.

V. CONCLUSION

In conclusion, we have calculated the classical and quantum properties of a HNLS and investigated its behavior for femtosecond pulses in optical fibers. Using the NBP we calculated the classical behavior directly for various parameters and found agreement with the exact analytical expression. We also use the NBP to show that on the distance scale of interest in the quantum analysis, the effects of the SSFS and other terms are not significant. We find that femtosecond solitons require a quadruple-clad fiber for propagation rather than the graded-index fiber traditionally used. The quantum analysis involved using the time-dependent Hartree approximation to calculate the QPD. The plots of the QPD showed self-squeezing with a distance scale influenced by the higher-order dispersion terms.

ACKNOWLEDGMENTS

This work was supported by the National Science Foundation through the Center for Telecommunications Research at Columbia University (F.S. and M.C.T.) and by the National Science Foundation through Grant No. ECS 89-21139 and the U.S. Army Research Office (M.J.P. and J.M.F.).

[1] A. Hasegawa and F. Tappert, Appl. Phys. Lett. **23**, 142 (1973).
[2] L. F. Mollenauer, R. H. Stolen, and J. P. Gordon, Phys. Rev. Lett. **45**, 1095 (1980).
[3] M. J. Potasek and B. Yurke, Phys. Rev. A **35**, 3974 (1987).
[4] P. D. Drummond and S. J. Carter, J. Opt. Soc. Am. B **4**, 1565 (1987).
[5] M. Rosenbluh and R. M. Shelby, Phys. Rev. Lett. **66**, 153 (1991).
[6] M. Kitagawa and Y. Yamamoto, Phys. Rev. A **34**, 3974

(1986).
[7] R. Tanas and S. Kielich, Opt. Commun. **45**, 351 (1983).
[8] T. A. B. Kennedy and P. D. Drummond, Phys. Rev. A **38**, 1319 (1988).
[9] B. Yurke and M. J. Potasek, J. Opt. Soc. Am. B **6**, 1227 (1989).
[10] Y. Lai and H. A. Haus, Phys. Rev. A **40**, 844 (1989); **40**, 854 (1989).
[11] E. M. Wright, Phys. Rev. A **43**, 3836 (1991).
[12] F. M. Mitschke and L. F. Mollenauer, Opt. Lett. **13**, 407 (1987); M. N. Islam, E. R. Sunderman, C. E. Soccolick, I. Bar-Joseph, N. Sauer, T. Y. Chang, and B. I. Miller, IEEE J. Quantum Electron. **25**, 2454 (1989).
[13] F. M. Sears, L. G. Cohen, and J. Stone, J. Lightwave Technol. **LT-2**, 181 (1984).
[14] R. Hirota, J. Math. Phys. **14**, 805 (1973).
[15] M. J. Potasek, J. Appl. Phys. **65**, 941 (1989).
[16] J. P. Gordon, Opt. Lett. **11**, 662 (1986).
[17] F. M. Mitschke and L. F. Mollenauer, Opt. Lett. **11**, 659 (1986).
[18] F. Singer, M. J. Potasek, and M. C. Teich, Quantum Opt.: J. Eur. Opt. Soc. B **4**, 157 (1992).
[19] B. Yoon and J. W. Negele, Phys. Rev. A **16**, 1451 (1977).
[20] M. J. Potasek, J. M. Fang, and M. Tabor (unpublished).
[21] K. J. Blow, N. J. Doran, and D. Wood, J. Opt. Soc. Am. B **5**, 1301 (1988).
[22] K. Kurokawa and M. Nakazawa, Appl. Phys. Lett. **58**, 2871 (1991).
[23] S. J. Carter and P. D. Drummond, Phys. Rev. Lett. **67**, 3757 (1991).